



HAL
open science

New Insights into Urea Electro-Oxidation: Complete Mass-Balances and Proof of Concept with Real-Matrix Effluent

Guillaume Hopsort, Laure Latapie, Karine Groenen Serrano, Karine Loubière, Theodore Tzedakis

► **To cite this version:**

Guillaume Hopsort, Laure Latapie, Karine Groenen Serrano, Karine Loubière, Theodore Tzedakis. New Insights into Urea Electro-Oxidation: Complete Mass-Balances and Proof of Concept with Real-Matrix Effluent. *Journal of The Electrochemical Society*, 2023, 170, pp.093507. 10.1149/1945-7111/acf87e . hal-04209320

HAL Id: hal-04209320

<https://ut3-toulouseinp.hal.science/hal-04209320>

Submitted on 17 Sep 2023

HAL is a multi-disciplinary open access archive for the deposit and dissemination of scientific research documents, whether they are published or not. The documents may come from teaching and research institutions in France or abroad, or from public or private research centers.

L'archive ouverte pluridisciplinaire **HAL**, est destinée au dépôt et à la diffusion de documents scientifiques de niveau recherche, publiés ou non, émanant des établissements d'enseignement et de recherche français ou étrangers, des laboratoires publics ou privés.

New insights into urea electro-oxidation: complete mass-balances and proof of concept with real-matrix effluent

Guillaume Hopsort^z, Laure Latapie, Karine Groenen Serrano, Karine Loubière and Theodore Tzedakis^z

^zCorresponding Author E-mail Address [guillaume.hopsort@univ-tlse3.fr][theodore.tzedakis@univ-tlse3.fr]

Laboratoire de Génie Chimique, Université de Toulouse, CNRS, INPT, UPS, Toulouse, France

KEYWORDS: Urea electro-oxidation (UEO); urine electrolysis; complete by-products analysis.

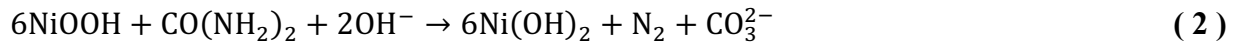
ABSTRACT

In the present work, all the by-products formed during the urea electrooxidation (UEO) by Ni(III) in alkaline medium are identified and quantified for the first time (*e.g.*, OCN^- , CO_3^{2-} , NH_4^+ , N_2 , NO_2^-). Complete mass balances are simultaneously established in both aqueous and gas phases for large urea conversion rates (>80%). The results provide clear evidence (with a maximal deviation of 2%) that, in addition to N_2 , N-overoxidized by-products are produced during the UEO. Electrolyses conducted with human urine samples under identical operating conditions result in different distributions of N and C-by-products. In particular, the formation of formic and oxalic acids in these latter experiments suggests the presence of different and/or additional mechanistic pathways during the UEO process. The amount of H_2 generated at the cathode is also quantified, showing a reduction of 30% in energy consumption when compared with water electrolysis. Finally, this study assesses the energy efficiency of UEO with urea synthetic and real-matrix effluents, thereby contributing to the development of this sustainable process, which enables energy recovery from waste.

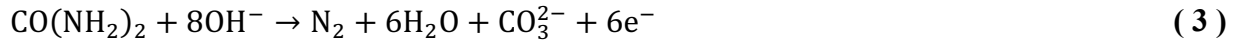
1. INTRODUCTION

The urea electro-oxidation (UEO) has been studied for the past 50 years, beginning with pioneering work in a neutral medium in the 1970s¹, with a view towards urine degradation. The industrial scaling of such a process is anticipated in alkaline media², primarily due to (i) the use of low-cost electrode materials and (ii) the cathodic generation of valuable H₂. Nickel-based anodes have been shown to possess the best electrocatalytic activity³ against the UEO. In particular, this UEO takes place on the Ni electrode at 0.55 V (vs. Hg/HgO)⁴, a value of ~ 0.1 V lower than the one observed on Pt-Ir⁵, Pt⁶, or Rh⁷ electrodes. It is well admitted that the overall electrooxidation pathway is indirect as described in **Eqs. (1)-(4)**.

At the anode:



Anodic overall:



Overall cell:



For a long time, the process was considered as an efficient solution for the anodic treatment of urea-containing effluents, mainly because (i) only the anodic formation of N₂, O₂, CO₂ was reported and (ii) the process generates gaseous H₂ at the cathode. According to several research works^{8,9}, the UEO process could thus solve some contemporary environmental challenges. Nevertheless, the issue related to the by-products formed was rarely addressed, thus creating a significant gap in the fundamental understanding of the reaction mechanism¹⁰. However, since 2018, five research papers have reported the occurrence of several by-products in the liquid phase: OCN⁻, NO_x⁻ (x = 2 and/or 3), NH₃ and CO₂ (identified as carbonate under alkaline medium)¹¹⁻¹⁵. All of these studies show an over-oxidation of the nitrogen (N) derived from urea, favoring the

formation of nitrite (oxidation state of N(+III)) at the expense of gaseous nitrogen (oxidation state of N(0)). Unfortunately, in the case of electrolysis with large urea conversion rates, complete mass balances (MB) are still scarcely established, even if complex mechanisms are always suggested^{12,13,15,16}. Identifying all the by-products requires the coupling of several analytical techniques, which is generally not done. Li et al¹² have revealed that the commonly used nickel-based catalysts exhibit a tendency to over-oxidize urea into NO_2^- with about 80% of Faraday efficiency (FE). Additionally, trace quantities of NO_3^- and N_2O , which could be harmful to the environment, have been detected. Tatarchuk et al¹³ have presented the UEO as an efficient pathway to both remove nitrogen waste and produce renewable fuels; they mentioned an urea overoxidation into NO_x^- (instead of the desired N_2) at $\text{Ni}(\text{OH})_2$ -based anodes, without fully clarifying the mechanism. They have also observed that UEO on $\text{Ni}(\text{OH})_2$ forms cyanate. The selectivity of the reaction can be oriented towards the N_2 production by modifying the nickel-based catalyst composition; for example, adding copper to the catalyst ($\text{Ni}_{0.8}\text{Cu}_{0.2}(\text{OH})_2$) increases the faradaic efficiency of N_2 from 30% to 55% at the same applied potential (e.g., 1.4 V vs. RHE at pH = 14)¹³. Chen et al¹⁵ have investigated the mechanisms of UEO by implementing electrochemical (EC) and Raman analyses. This study has deciphered the mechanism transforming nitrogenous nucleophile into the Nitrogen Oxidation Reaction (NOR) mediated by the $\beta - \text{Ni}(\text{OH})_2$ electrode. In particular, a two-step NOR is proposed, involving a proton-coupled electron transfer (PCET) bridging dehydrogenation and nucleophile dehydrogenative oxidation. Despite these major advances in the understanding of the UEO mechanism, no complete mass balance is established in these works. Faraday efficiency balances are always reported, but their scope remains limited as, without complete mass balances, the composition of liquid and gaseous phases cannot be fully determined. In previous works^{11,16}, we proposed for the first time a complete mass balance in the liquid phase

during potentiostatic electrolyzes obtained at high urea conversion rates (>80%); as well as kinetics laws and reaction mechanisms based on a chain of reactional adsorption of urea on Ni(III) active sites. However, in this study, no mass balance in the gas phase has been made, thus pointing out the need of additional investigation for the part of the mechanism leading to the gaseous products.

Some works have reported electrolyzes on real human urine electrolysis by using BiO_x-TiO₂¹⁷ or IrO₂¹⁸ anodes. However, to the best of our knowledge, none exists with nickel electrode and real human urine previously alkalized. Such lack makes difficult to validate the efficiency of the UEO processes with real effluents in a view of a future industrial implementation.

To fill this gap, the present study aims at elucidating the performances of a lab-scale EC reactor operating with real human urine and at rigorously comparing them to the ones in presence of urea synthetic solutions. For this purpose, the analytical methods need to be optimized so as to perform complete analysis of all electrogenerated adducts in both aqueous and gaseous phases. This preliminary study will thus pave the way for operating the process at larger scale.

2. EXPERIMENTAL INFORMATION

2.1 Material and methods

Chronoamperometry experiments were performed at 0.55 V vs. Hg/HgO. At this potential, our previous work¹¹ showed by voltammetry studies that the current achieved a plateau caused by the urea mass transfer limitation of the urea-catalyzed oxidation of Ni(OH)₂ to NiOOH. Electrolyzes were performed under Ar-controlled atmosphere (1.5 L.h⁻¹) by using a PGSTAT128N potentiostat (Metrohm, Switzerland). Schematically represented in **ESI 1**, a H-type EC cell divided by an anionic membrane (IONAC MA-375, Lanxess, Germany) was used and operated at room

temperature. A nickel plate electrode (28 cm²) was used as the working electrode (anode) and a Hg/HgO electrode (with 1 mol.L⁻¹ KOH), immersed into the stirred anolyte (60 cm³), served as reference. A platinum plate was employed as counter electrode in catholyte (60 cm³). All chemicals were supplied from Sigma-Aldrich (USA). Ultra-pure water (18 MΩ.cm) was systematically used and all the solutions were prepared at a KOH concentration of 1 mol.L⁻¹ (alkaline medium at pH 14). Human urine samples were obtained from two healthy male volunteers (aged between 25 and 30 years old). The entire sample of urine was stored at 4 °C between experiments. All assays were duplicated using the same batch of urine to ensure repeatability.

2.2 Analytical procedures

Electrolytes were analyzed by ion chromatography (IC) and mass spectroscopy (MS) according to a previously developed method¹⁹, reminded in **ESI 2**. Typical chromatograms and calibration curves of formic acid (FA) and oxalic acid (OA) are respectively shown in **ESI 3 and ESI 4**.

Care was taken to ensure that no nitrogenous or carbonaceous compounds present in the anolyte migrated to the catholyte via the IONAC anionic separator used (the composition of the catholyte was analyzed at the end of the electrolyzes).

Total organic carbon (TOC) was measured using a SHIMADZU TOC-L apparatus. The applied method was detailed in our previous work¹¹.

A Varian 450-GC gas chromatograph (GC) was used to quantify the composition of the gas phase (Haysep N 80/100 Mesh, Haysep Q 80/100, Molsieve 13X, oven temperature 50 °C, Thermal Conductivity Detector (TCD), carrier gas Ar, injector temperature 140 °C and TCD temperature 200°C). Typical chromatograms and calibration curves for N₂, O₂ and H₂ are presented in **ESI 5** and **ESI 6**.

Since the electrolysis was performed in a divided cell, the sole cathodic reaction involved is the reduction of water to H₂. As a consequence, the amount of H₂ formed, n_{H₂} (mol), corresponded to the one supplied by the **Eq. (5)**.

$$n_{\text{H}_2} = \frac{Q_{\text{total}}}{\mathcal{F} \times 2} \quad (5)$$

where \mathcal{F} is the Faraday constant (C.mol⁻¹), and Q_{total} represents the total charge supplied to the EC cell. Q_{total} was calculated by integrating the current I(t) obtained at the applied potential of 0.55 V vs. Hg/HgO with time during chronoamperometry measurements.

2.3 Faraday efficiency

The Faraday efficiency of the compound i, represented as FE_i (%), was defined by **Eq. (6)**.

$$\text{FE}_i = \frac{n_i \times n_e \times \mathcal{F}}{Q_{\text{total}}} \times 100 \quad (6)$$

where n_i is the amount of the compound i (mol) and n_e represents the number of electrons exchanged (dimensionless) which was equal to:

- 1 for OCN⁻ and NH₄⁺ (the formation of these species indirectly implies Ni(II)→Ni(III) oxidation system, as described in a previous work¹⁶),
- 6 for N₂ and
- 6 for NO₂⁻.

2.4 Energy of the EC cell

The energy consumption of the EC cell, denoted as E_{consumed} (Wh), was defined by **Eq. (7)**.

$$E_{\text{consumed}}(t) = \int_0^t I(t) \times \Delta V(t) \times dt \quad (7)$$

where ΔV is the cell voltage (V).

The energy related to the H₂ produced, denoted as E_{eq. H₂ produced} and expressed in kWh, can be calculated using **Eq. (8)**.

$$E_{\text{eq. H}_2 \text{ produced}} = V_{\text{H}_2, \text{produced}} \times \rho_{\text{H}_2, (\text{STP})} \times \lambda_{\text{H}_2} \quad (8)$$

where V_{H₂,produced} was the total amount of H₂ formed during electrolysis (L) and ρ_{H₂} the volumetric density of hydrogen in standard temperature and pressure (STP) conditions which was evaluated at 8.4×10⁻⁵ kg.L⁻¹ ²⁰. At 25°C and under atmospheric pressure, the H₂ mass-energy density λ_{H₂} is reported equal to 33.33 kWh.kg_{H₂}⁻¹ ²¹. This parameter represents an estimate of the energy that would be produced if H₂ was completely combusted.

In order to estimate the overall energy consumption of the process, the actual consumption, ΔE (Wh), was then expressed according to **Eq. (9)**.

$$\Delta E = E_{\text{consumed}} - E_{\text{eq. H}_2 \text{ produced}} \quad (9)$$

3. RESULTS AND DISCUSSION

3.1 Urea synthetic electrolysis

The first set of experiments concerns the performance of chronoamperometry electrolysis of a urea solution at 0.55 V vs. Hg/HgO.

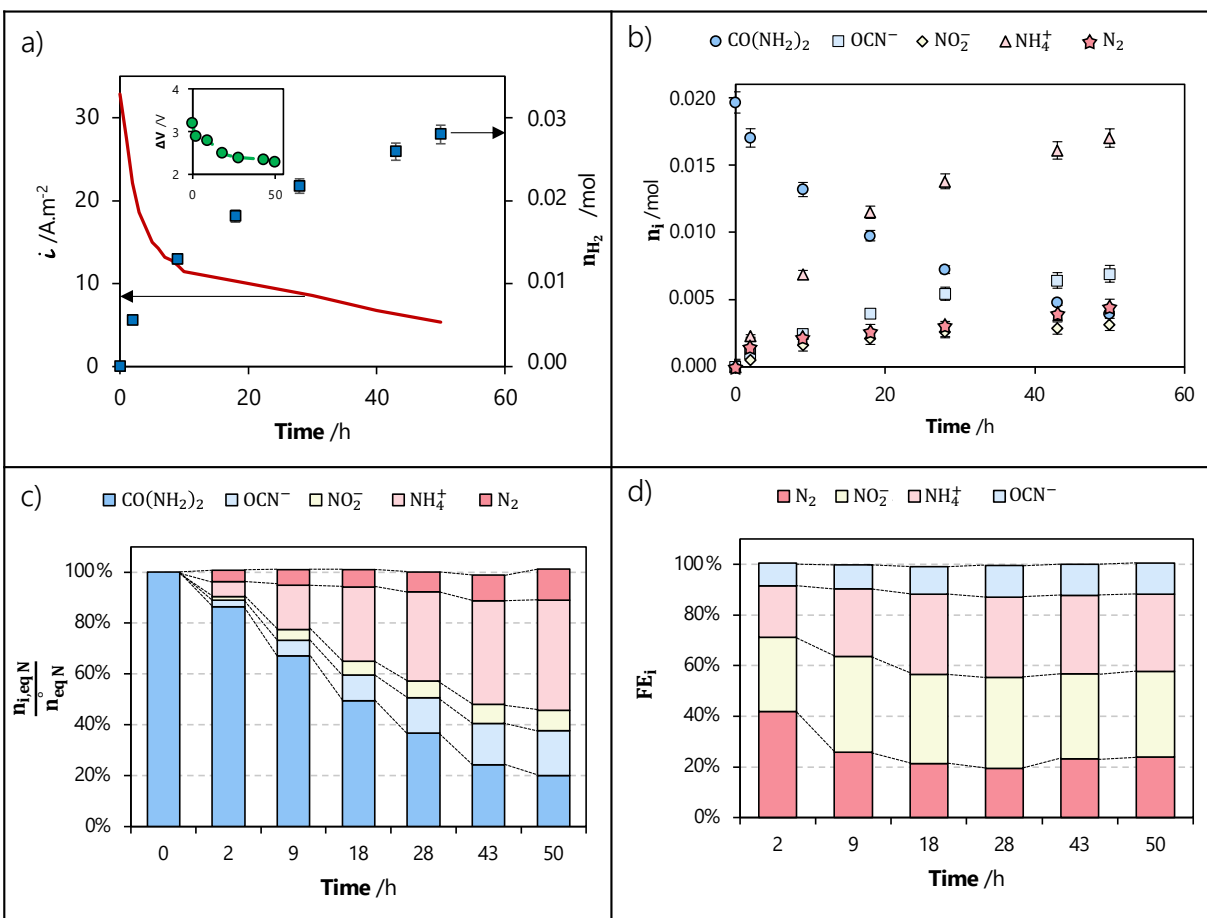


Figure 1. Typical results obtained from chronoamperometric electrolysis of a urea synthetic solution (0.33 mol.L⁻¹) in alkaline medium (1 mol.L⁻¹ KOH): a) current density and the amount of formed H_2 (*inset*: cell voltage), b) temporal profiles of molar quantity of identified N-species, c) N-mass balance, and d) N-Faraday efficiency balance.

Figure 1-a illustrates the temporal evolution of the UEO current density, with the cell voltage shown in the inset. The observed decrease in cell voltage (from 3.1 V to 2.2 V) is attributed to both a decrease in cathodic overvoltage and an ohmic drop. **Figure 1-b** reports the temporal profiles of the number of moles for each identified N-specie (the raw data are provided in **ESI 7**). The urea degradation achieves a conversion rate of 80% over 50 h, predominantly forming NH_3 (at 43%, observed as NH_4^+ in IC analysis). By bubbling the gases anodically formed in an acid solution (HCl), it was verified that no trace of gaseous ammonia was present, and thus that all the ammonia

formed remained dissolved in the solution. A simultaneous evolution was observed with the current density (**Figure 1-a**), thus confirming the absence of poisoning phenomena during the electrolysis.

Figure 1-c presents, for the first time, a complete mass balance (MB) of the N-species formed in both liquid and gas phases. Interestingly and unequivocally, OCN^- , NO_2^- , NH_3 and N_2 are the main (> 98%) N-compounds produced during the electrolysis since the sum of their molar quantities remains equal to the N-amount initially present in the EC cell ($2 \times$ initial moles of urea), and this whatever the electrolysis time. As mentioned by Hopsort et al.¹¹ and illustrated in **ESI 8**, the MB of the C-species (namely $\text{CO}(\text{NH}_2)_2$, OCN^- and CO_3^{2-}) is also validated (more than 98%).

Figure 1-d reports the faradaic efficiency for all the identified N-compounds. The total FE_i reaches 100% (with a maximal deviation of 2%), showing that the charge balance is validated for 50 hours. The following conclusions can be drawn:

- (i) After 9 hours of electrolysis (corresponding to the disappearance of 35% of the urea initially present), the distribution of the concentrations of the various compounds does not evolve anymore (*i.e.*, their FE_i tends to become constant). Such trend could be explained as follows. Urea is oxidized according to a pathway that produces intermediate products as well as nitrites. These intermediates accumulate over time and, once enough concentrated in the medium, would oxidize into nitrites. Then, the ratio of the number of electrons released for nitrite formation to the total electrons remains constant, as far as the urea is consumed. Once the main pathways for urea oxidation and by-product formation are established - by setting up the indirect massive nickel electrode process ($\text{Ni}(0) \rightarrow \text{Ni}(\text{II}) \rightarrow \text{Ni}(\text{III})$) - a constant pattern emerges. The ratio of the molar

fluxes formed by each reaction pathway, and thus the related FE_i , remains constant, regardless of the residual urea concentration.

- (ii) Between the four detected products (**Figure 1-d**), only N_2 and NO_2^- exhibit a higher oxidation state of nitrogen (0 and +III respectively) compared to urea (-III). Together they represent more than 60% of the total charge. The N-oxidation state for the two other compounds (NH_4^+ and OCN^- , both at (-III)) does not change, which is in agreement with the previously presented mechanism¹⁶. The formation of these compounds (NH_4^+ and OCN^-) results from a catalytic reaction of Ni(III) with urea, which requires the prior formation of Ni(III) from the oxidation of Ni(II) with an exchange of an electron. By applying $n_e = 1$, according to the Ni(II)→Ni(III) oxidation reaction, the Faraday efficiency balance is validated, thus indirectly confirming the previous mechanism¹⁶.
- (iii) Unfortunately, the formation of OCN^- and NO_2^- occurs to the detriment of N_2 , thus making the process less interesting from a sustainable point of view. To overcome this issue, several attempts are very recently made to orient the mechanism towards N_2 , for example by electrode material functionalization^{14,22}.

The production of H_2 estimated from **Eq. (5)** is reported in **Figure 1-a**, leading to a value of 1.78 $mol_{H_2} \cdot mol_{urea}^{-1}$ after 50 hours of electrolysis. This means that, overall, the oxidation of 1 mole of urea releases 3.5 electrons, instead of the 6 electrons expected for the generation of 1 mole of N_2 .

Finally, in this section, the by-products of the urea synthetic electro-oxidation were identified and quantified, demonstrating that less than 30% of the urea was converted into N_2 .

3.2 Electrolysis of human urine

The industrial development of EC processes inevitably involves the trial phase with real matrices of urea. In this section, the UEO will be studied, with human urine previously alkalinized, during chronoamperometry electrolysis.

3.2.1 Effect of alkalinization

Urine was alkalinized by adding KOH pellets (until reaching $\text{pH} = 14$ or 1 mol.L^{-1}), and the effect of this alkalinization on the concentration of the major compounds contained in urine was examined. The results are shown in **Table 2**.

Two phenomena can be noticed:

- (i) The alkalinization of urine solutions results in the precipitation of a whitish solid which has been characterized by optical microscopy and ICP-OES analysis (see **ESI 9**). Some of the mineral salts identified are whewellite ($\text{Ca}(\text{C}_2\text{O}_4) \cdot \text{H}_2\text{O}$) and struvite ($\text{NH}_4\text{MgPO}_4 \cdot 6\text{H}_2\text{O}$)²³. The ICP-OES analysis of the precipitate has confirmed such trends by revealing that the elements Ca (7.3 wt%), Mg (16.0 wt%) and P (3.8 wt%) are present in majority.
- (ii) The degradation of organic matter (*i.e.*, 7% decrease in TOC) caused by the alkalinization of the biological solution leads to an increase in the concentrations of NH_3 (+42%), oxalic acid (+23%) and the appearance of formic acid. Note that the formation of low-molecular-weight organic acids (LMWOA), such as FA and OA, has been already observed²⁴ during the alkalinization of water from a brown water lake.

3.2.2 Chronoamperometry results

Figure 2 presents the results related to electrolysis at constant potential (0.55 vs. Hg/HgO) carried out with freshly excreted urine solution after alkalinization. Note that the corresponding urea

concentration in the urine was measured at 0.23 mol.L^{-1} (equivalent to 42% of TOC measured), a value lower than the generally admitted urea concentration into the urine (*i.e.*, 0.33 mol.L^{-1}).

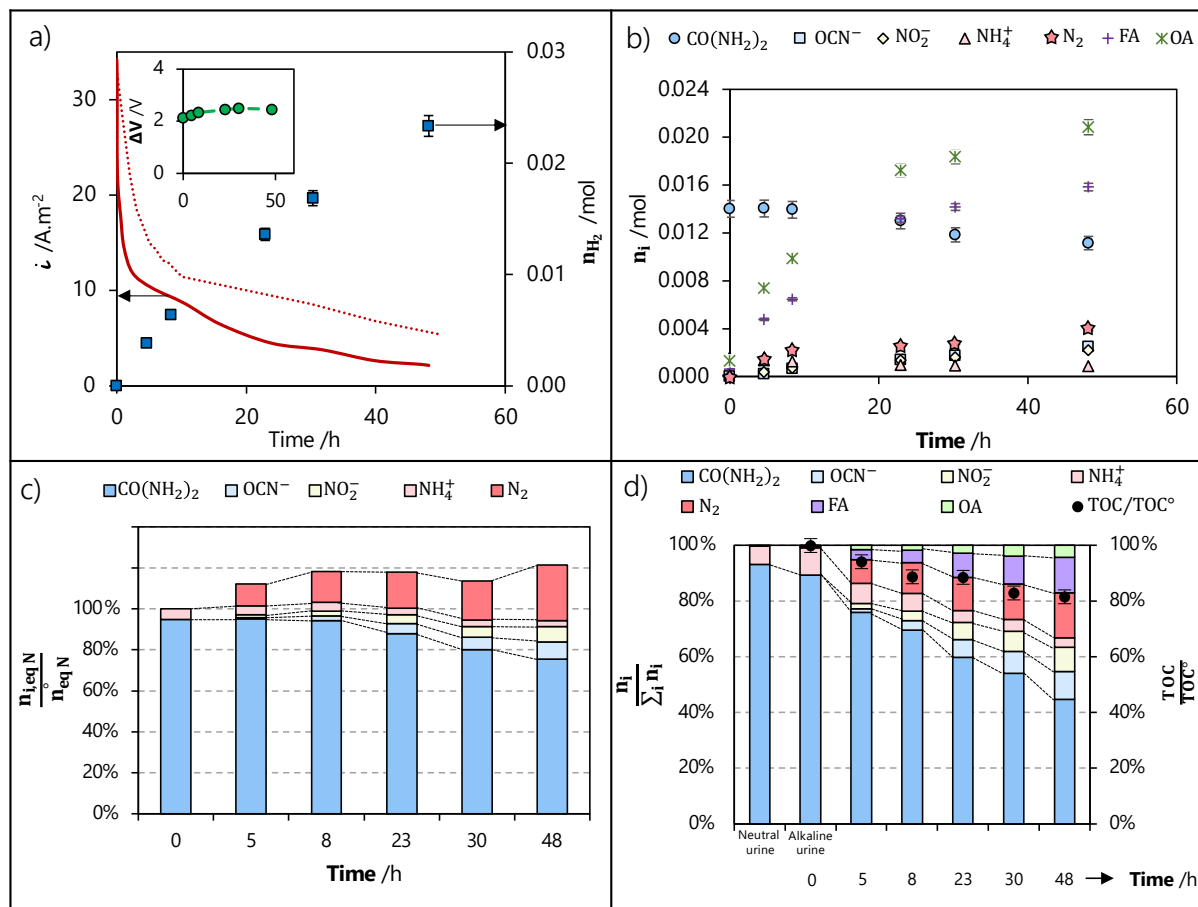


Figure 2. Typical results obtained from chronoamperometric electrolysis of a human urine solution in alkaline medium ($1 \text{ mol.L}^{-1} \text{ KOH}$): a) time profiles of the current density (dashed line corresponds to urea synthetic solution, reported in **Figure 1**) and the formed H_2 amount (*inset*: cell voltage), b) temporal profiles of molar quantity of *identified* species, c) urea-mass balance and d) amount-proportions of *identified* substances in the urine.

Figure 2-a presents the temporal evolutions of the current density during electrolysis of both (i) urea synthetic (dashed line extracted from **Figure 1**) and (ii) human urine (solid line) solutions. The initial current density value, after immediate polarization, is higher for urine electrolysis (34 A.m^{-2} with urea concentration of 0.23 mol.L^{-1}) than urea synthetic solution (31 A.m^{-2} with urea

concentration of 0.33 mol.L^{-1}), thus suggesting an EC activity at the applied potential other than the one observed between urea and $\text{Ni(III)} \rightarrow \text{Ni(II)}$ redox system. This additional activity could be direct or indirect, and would involve other organic molecules present into the urine, as already depicted for creatinine²⁵ or ascorbic /uric acids and glucose²⁶.

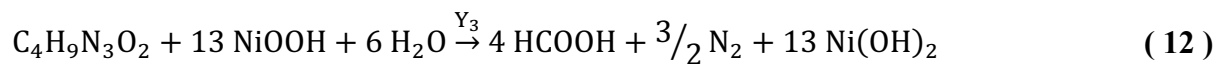
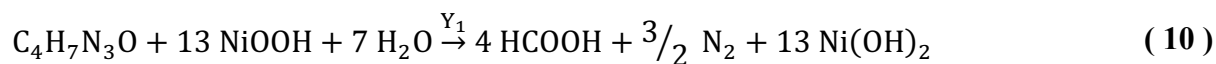
Immediately after the start of urine electrolysis, the current density decreases more rapidly over time than it does during urea synthetic electrolysis. However, the same type of temporal evolution was observed for both electrolyses.

Figure 2-b presents the temporal evolution of the molar quantity of the urea in the case of the urine electrolysis under the applied potential. The molar quantity reduces from 0.014 moles to 0.010 moles after 50 h of electrolysis, resulting a low conversion.

Table 1 compares the temporal trends, after 50 hours of electrolysis, in terms of (i) urea conversion rate X (for urea synthetic electrolysis in **Figure 1-b**) and for urine electrolysis in **Figure 2-b**) and (ii) current density i . These results show that:

- (i) in the case of the urine, the current decreases and the consumption of the urea remains low ($X < 20 \%$);
- (ii) it cannot be ruled out that the degradation of urea might be induced by other oxidizing molecules (such as hypochlorite²⁷) produced by electrooxidation;
- (iii) as indicated above, the measured current concerns the urea oxidation as well as organic molecules;
- (iv) the species present in urine seems to limit the UEO without inhibiting it. Indeed, even if the measured currents remain significant, higher values could be expected taking into account the urea residual concentrations. This would suggest a competition between urea and other organic molecules present into the urine against the nickel sites.

Figure 2-b also presents the temporal variation of the molar amount of the products detected during the urine electrolysis. The by-products (OCN^- , NO_2^- , NH_3 , N_2) observed during the UEO are still present (for more details, **ESI 10** provides raw data (molar amount) of all the reactants and adducts present in the process against time and charge). However, their quantities remain lower compared to the ones detected in the case of urea, which is in agreement with the low urea conversion rates. Besides, supplementary products are detected and in relatively significant quantities: typically, formic acid and oxalic acid achieve 0.016 and 0.02 moles after 50 hours respectively. These quantities are higher than the initial urea molar quantity observed into the urine, thus suggesting an electrogeneration of these acids by oxidation of another organic molecule. Organic molecules (such as creatinine $\text{C}_4\text{H}_7\text{N}_3\text{O}$, creatine $\text{C}_4\text{H}_9\text{N}_3\text{O}_2$, etc) electrooxidation could generate FA (HCOOH) and OA (HOCCOOH) with possible reactions described by **Eqs. (10)-(13)**.



where Y_i could be a catalyst or complexing agent present in the matrix.

In order to gain a more precise understanding of the formation of these by-products, a further representation has been provided in **Figure 2-c**, where the mass balance of five nitrogenous by-products (including urea) is presented over the electrolysis time. On the y-axis, it has been chosen to plot the ratio of the molar amount of compound i by the total molar amount of nitrogenous

compounds initially detected. Note that larger nitrogenous molecules (creatinine, creatine, glycine, etc.) cannot be included, as they have not been titrated. The nitrogenous by-products monitored can be released by both UEO and electrooxidation of the larger molecules, thus explaining why the total molar ratio are greater than 100 %. This result indirectly demonstrates the electro-oxidation of molecules such as creatinine and creatine, and/or the competition existing between UEO and the electro-oxidation of these molecules. Some previous works have already pointed out this production, such as the formation of cyanate from the oxidation of glycine²⁸ or the N₂ generated by the oxidation of creatinine^{25,29}.

Figure 2-d shows the molar distribution of the *identified* species present in the matrix. The term $\sum_i n_i$ represents the sum of the moles of the seven identified and quantified compounds in the mixture (provided values in **ESI 10**).

First, one can observed that FA appears through simple alkalization which could be due to chemical reactions involving (i) urea or another organic compound and dissolved oxygen, or (ii) even another oxidizers present into urine^{30,31}. The rise of temperature during the alkalization step could catalyze this reaction³².

All these findings clearly demonstrate that the matrix has a significant effect to orientate the products of the UEO, typically to obtain FA and OA instead of carbonate (as identified in the case of urea synthetic electrolysis).

Simultaneously to the electrolysis, 60 mL of alkalized urine have been stored at room temperature and the concentration of the various species monitored. For comparison's purposes, no degradation of organic matter is observed after alkalization and without applying potential in alkaline and neutral urine solutions (the amounts of initial and final urea/FA/OA have been measured and remain constant).

As also observed in **Figure 2-d**, nitrite accounts for 4 *mol.*% of the total substance amount at the end of electrolysis, while it represents 7 *mol.*% in the case of urea synthetic solution (**ESI 7**). The same trends are observed for ammonia with 38 *mol.*% being produced in the case of urea synthetic electrolysis compared to 1.5 *mol.*% for urine electrolysis (already present in the initial sample); and cyanate where 4.3 *mol.*% with urine *vs.* 15 *mol.*% with urea were obtained at the end.

As a reminder, about 3,000 compounds have been identified in urine, according to Bouatra et al³³, and are estimated to represent more than 42% of the initial measured TOC, as presented in **ESI 11**. The presence of organic molecules other than urea can cause significant modifications of these proportions. Indeed, these compounds can exhibit an electrocatalytic behavior against nickel (FA³⁴, dopamine³⁵, glucose³⁶, etc), and thus possibly presenting oxidative behavior against the urea electrogenerated adducts.

The reactions delineated in **Eqs. (10)-(13)** involve the usage of nickel(III) sites between 13 and 17 times, corresponding to the exchange of 13 to 17 electrons. This results in the release of approximately 3.3 to 4.3 electrons per mole of carbon, depending on the nature of the products. For comparison, the hydrogen production occurring during the electrolysis of urea synthetic involves 3.5 electrons for oxidizing one mole of carbon urea. This data provides further evidence for the matrix effect: the presence of other organic molecules in urine, such as creatinine and creatine, alters the urea degradation pathway established with synthetic solution.

The electro-oxidation of organic molecules, which involves such a high number of electron exchanges, can be explained by the continuous electro-regeneration of the active nickel(III) adsorption sites. These molecules are strongly adsorbed onto these sites. This result confirms the indirect electro-oxidation of organic molecules on nickel sites.

In addition, the adsorption on nickel sites of higher size organic molecules (such as creatinine²⁵), limits the urea adsorption on these nickel sites and consequently completely modifies the reaction pathway.

3.2.3 Creatinine electrolysis

The objective of this new set of experiments is to elucidate the EC behavior of creatinine. For that, chronoamperometry electrolysis of a creatinine solution was performed for 40 hours in the undivided EC lab-cell described by Hopsort et al.¹¹, in which a massive nickel electrode (18 cm², single face) was used and an applied potential of 0.55 V vs. Hg/HgO. The concentration of creatinine was chosen to be close to the maximal physiological concentration (*i.e.*, the maximal concentration encountered in human urine), namely 0.013 mol.L⁻¹. The results (based on the monitoring of the liquid phase only) are shown in **Figure 3**.

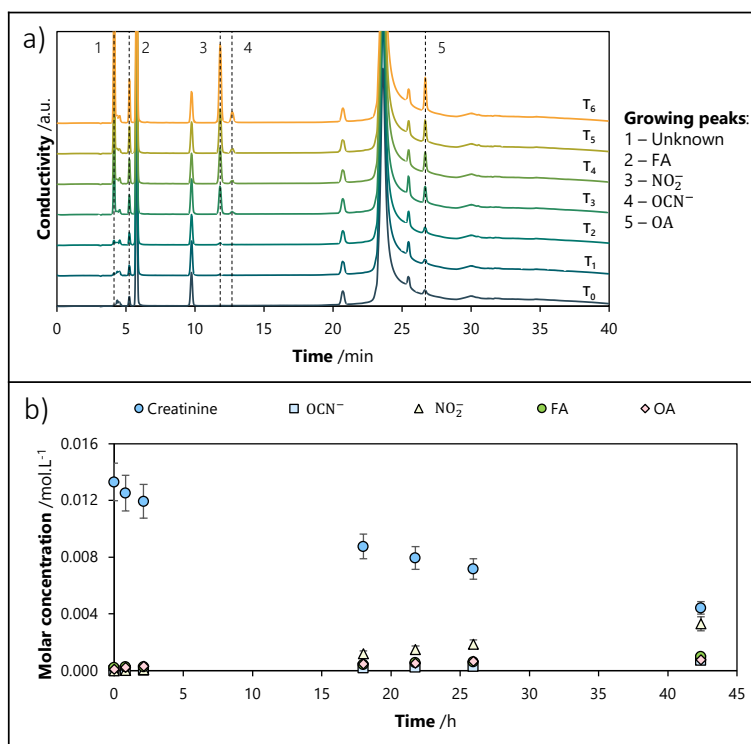


Figure 3. Results of chronoamperometry of a creatinine solution (0.013 mol.L^{-1}) on nickel electrode (18 cm^2) in alkaline solution ($\text{KOH } 1 \text{ mol.L}^{-1}$): temporal profiles of a) the anion chromatograms, and b) concentration of creatinine and *identified* by-products.

Several observations can be drawn from these results.

In order to determine if creatinine was oxidized, the reaction medium was sampled over time, and analyzed by ion chromatography. **Figure 3-a** shows the results only on the anion side (no change being observed on the cation side). It can be observed that the amount of 5 compounds increases: (i) FA, (ii) nitrite, (iii) cyanate, (iv) oxalic acid and (v) an unidentified molecule. The creatinine signal measured by MS reveals a degradation of 67 % at the end of electrolysis.

The temporal variations of both reagent and product concentrations in the bulk are provided in **Figure 3-b** which confirms the degradation of creatinine under these pH conditions and on nickel electrodes.

All these findings support the idea that:

- (i) during the electrolysis of urine solution (as presented in the previous section), a competition for accessing to active nickel(III) sites takes place between urea (the main compound in urine) and creatinine (the second abundant compound in urine). To go further, more investigations on the relative degradation rate for each molecule need to be done.
- (ii) the formation of oxalic and formic acids, observed during the electrolysis of urine (and not with urea), could be induced by the creatinine electro-oxidation.

3.3 Energy cost assessments of urea and urine electrolysis

The energy consumption of electrolysis is here compared with (i) urea synthetic and (ii) urine.

For urea synthetic electrolysis, **Figure 4-a** shows that after 50 hours of electrolysis, the UEO process consumes 34 kWh of electricity to produce 1 kg of H₂. This value has the same order of magnitude as the one reported by Boggs et al² in 2009 (38 kWh.kg_{H₂}⁻¹) who carried out chronoamperometric measurements under severe conditions of alkalinity (at 1.4 V vs. Hg/HgO and 5 mol.L⁻¹ KOH).

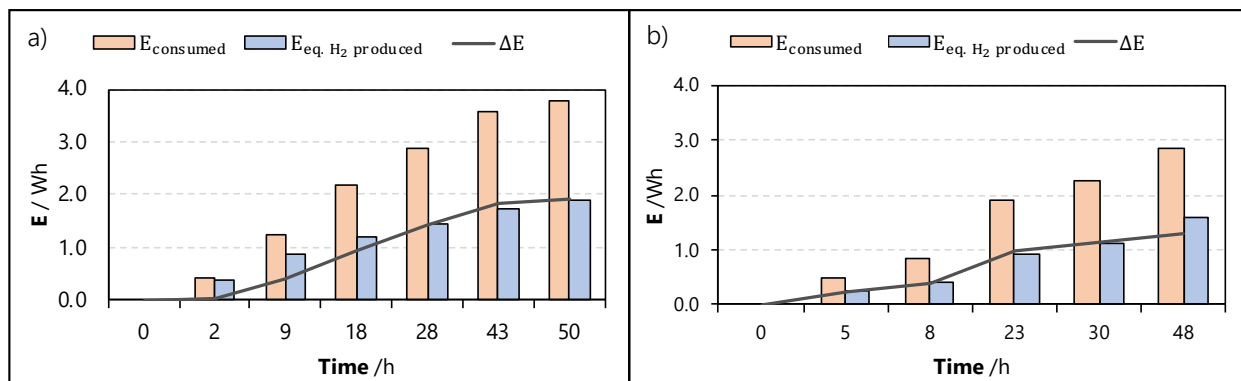


Figure 4. Energy data corresponding to the EC-cell consumption, the equivalent energy resulting from H₂ production, and the deviation between the consumption and the added-value energy during the UEO electro-oxidation in the case of a) urea synthetic and b) urine electrolyses.

In the case of urine electrolysis (**Figure 4-b**), as time progresses, the energy consumed by the system increases until reaching 2.9 Wh. Similar to the energy consumption, the energy equivalent of H₂ increases in the same manner up to 1.6 Wh, resulting in an energy differential (ΔE) of 1.3 Wh. Given the total amount of hydrogen formed during electrolysis (*i.e.* 2.34×10^{-2} mol, **Figure 2-a**), the energy consumption for urine treatment is 28 kWh. kg_{H₂}⁻¹, and thus reduced by 18% when compared to the electrolysis of urea (34 kWh. kg_{H₂}⁻¹). However, this consumption remains almost 30% lower than the one required to obtain the same amount of H₂ from water electrolysis³⁷, assuming identical levels of purity and electrolyte alkalinity.

CONCLUSIONS

In this study, chronoamperometric electrolysis was carried out on urea synthetic and real human urine solutions comparatively to investigate and elucidate the formation of by-products of UEO in alkaline media on a Ni massive electrode.

Firstly, an analytical tool combining ion chromatography/mass spectroscopy and gas chromatography was developed, allowing monitoring of the concentration of reactants and adducts over the electrolysis time. During urea synthetic electrolysis, an 80% conversion rate was achieved over a period of 50 hours. A complete mass balance of the nitrogen compounds (CO(NH₂)₂, OCN⁻, NO₂⁻, NH₃, N₂) was performed for the first time. The sum of the concentrations of all the identified nitrogen by-products represented almost 98% of the initial N-urea involved. NH₃ was the predominant N-compound generated during the UEO and its content reached 43% of the initial

urea at the end of the electrolysis. The faradaic efficiency achieved 100%, thus validating the charge balance with a maximum deviation of 3.9 %. These quantitative mass and charge balances during electrolyzes with a significant conversion rate (>80%) thus allowed for the confirmation of the previously proposed reaction mechanism¹⁶. However, the formation of OCN^- and NO_2^- , at the expense of N_2 (which represented 23% of initial urea at the end of electrolysis) limited the environmental viability of the process. For further optimization of the process, the influence of the applied potential could be investigated in an attempt to promote the N_2 formation against NO_x -type products. The energy consumption for H_2 production, at the end of electrolysis, was quantified at $34 \text{ kWh} \cdot \text{kg}_{\text{H}_2}^{-1}$, and found comparable to previous works.

Secondly, with the aim of studying the behavior of human urine against a nickel anode, an alkalization step (until pH reached 14) was performed on human-volunteer urine solutions. The precipitation of organic matter and mineral salts (phosphorus, sulfur, calcium) in the form of whewellite or struvite was shown. The monitoring of molar amounts of *identified* species during urine electrolysis ($\text{CO}(\text{NH}_2)_2$, OCN^- , NO_2^- , NH_3 , N_2 , CO_2H_2 , $\text{C}_2\text{O}_4\text{H}_4$) revealed the occurrence of additional *unidentified* electroactive organic molecules in urine, that induced competition of the electroactive sites with urea and thus simultaneous and competitive reaction pathways. Indeed, the urea conversion rate was lower (20%) in comparison to the urea synthetic electrolysis (66%) when given the same amount of supplied charge (4500 C). The matrix composition of urine significantly influenced the product distribution, with the appearance of formic acid and oxalic acid during electrolysis. The formation of these acids was demonstrated by carrying out electrolysis of synthetic creatinine, suggesting some competition effects between the latter and urea for accessing to the active nickel(III) sites when electrolyzing real matrices. To that end, it could be interesting

in the future to study the influence of operating parameters (KOH concentration or applied potential) towards by-products electroactivity against nickel electrode.

Thirdly, the energy consumption of the process was monitored throughout the duration of the urine electrolysis. The energy consumption ($28 \text{ kWh} \cdot \text{kg}_{\text{H}_2}^{-1}$) was decreased by approximately 18% compared to urea synthetic electrolysis, thus highlighting the potential benefits of urine as a resource to produce H_2 by electrochemical processes. The electrolysis of a human urine solution was found to decrease the energy cost by 30% when compared to water electrolysis, making possible scaling-up of the process on pilot scale.

Finally, these findings emphasize the importance of considering the electrolyte composition and matrix effects when designing and optimizing EC systems for urea electrolysis. Further research is still needed to enhance the selectivity towards N_2 formation and to improve the energy efficiency of such processes. Overall, these results contribute to the understanding of EC urea degradation and pave the way for the development of more sustainable and efficient technologies for the utilization of urea and the treatment of urine.

TABLES.

Table 1. Comparison of conversion rates and current densities during chronoamperometric electrolysis at 0.55 V vs. Hg/HgO of (i) urea synthetic and (ii) urine solutions

| Electrolyzed solution | Urea conversion rates X (%) | Current density i (A.m ⁻²) |
|-----------------------|-----------------------------|--|
| Urea synthetic | 80 | $0.19 \times i^0$ |
| Urine | 20 | $0.07 \times i^0$ |

Table 2. Effect of the alkalization (pH = 6.2 and pH = 14 before and after alkalization respectively) on the main compounds in urine. The deviation values were calculated as the ratio of the difference between the concentrations before and after alkalization by the concentration before alkalization, namely as $(C_{i,before} - C_{i,after})/C_{i,before} \times 100$.

| | Analyte | | | | | | | | | | | |
|----------------------------|-----------------------------------|---|------------------------------|-------------------------------|-------------------------------|-----------------|------------------------------|-----------------|------------------|------------------|-----|-----|
| | $(mol.L^{-1} \pm 0.1).10^3$ | | | | | | | | | | | |
| | CO(NH ₂) ₂ | NO ₂ ⁻ | NO ₃ ⁻ | SO ₄ ²⁻ | PO ₄ ³⁻ | Cl ⁻ | NH ₄ ⁺ | Na ⁺ | Mg ²⁺ | Ca ²⁺ | FA | OA |
| Before alkalization | 248.8 | / | 1.4 | 12.0 | 18.0 | 85.8 | 17.8 | 104.3 | 4.0 | 3.0 | / | 0.7 |
| After alkalization | 233.6 | / | 1.3 | 11.4 | 15.1 | 82.9 | 25.3 | 104.3 | / | 2.8 | 1.6 | 0.9 |
| Deviation (%) | ↓7 | / | ↓7 | ↓5 | ↓16 | ↓3 | ↑42 | = | ↓ | ↓6 | ↑ | ↑28 |
| | $(g.L^{-1} \pm 0.1)$ | | | | | | | | | | | |
| | TOC | CO(NH ₂) ₂ (eq. C) | FA (eq. C) | OA (eq. C) | | | | | | | | |
| | Before alkalization | 7.1 | 3.0 | / | 0.017 | | | | | | | |
| | After alkalization | 6.6 | 2.8 | 0.019 | 0.020 | | | | | | | |
| | Deviation (%) | ↓7 | ↓7 | ↑ | ↑17 | | | | | | | |

ASSOCIATED CONTENT

Supporting Information. Additional figures including cell scheme, IC-MS procedure, typical IC and gas chromatograms, calibration curves and characterization of the precipitate obtained after the alkalization of urine are provided.

ACKNOWLEDGMENT

The authors would like to thank Elyes Piguet for his help to carry out the creatinine electrolysis experiments.

AUTHOR INFORMATION

Corresponding Author

PhD. applicant Guillaume Hopsort, Laboratoire de Génie Chimique, Université de Toulouse, CNRS, INPT, UPS, Toulouse, France ; ID ORCID <https://orcid.org/0000-0002-5619-9667> ;

Email: guillaume.hopsort@univ-tlse3.fr

Pr. Theodore Tzedakis, Laboratoire de Génie Chimique, Université de Toulouse, CNRS, INPT, UPS, Toulouse, France ; ID ORCID : <https://orcid.org/0000-0002-9222-4487> ; Email:

theodore.tzedakis@univ-tlse3.fr

Author Contributions

G. Hopsort: Conceptualization, Methodology, Validation, Formal analysis, Investigation, Resources, Data curation, Writing – Original Draft, Visualization; *L. Latapie*: Formal analysis, Resources; *K. Groenen Serrano*: Conceptualization, Writing – Review & Editing, Supervision; *K. Loubière*: Conceptualization, Writing – Review & Editing, Supervision; *T. Tzedakis*:

Conceptualization, Writing – Review & Editing, Supervision, Project administration, Funding acquisition.

Funding Sources

This work was supported by the French National Research Agency (proposal [HYUREA ANR-19-CE04-0009](#)).

NOTES

The authors declare no competing financial interest.

ABBREVIATIONS

EC: ElectroChemical; FA: Formic Acid; GC: Gas Chromatograph; IC: Ion Chromatography; ICP-OES: Inductively Coupled Plasma Optical Emission Spectroscopy; LMWOA: Low-Molecular-Weight Organic Acid; MB: Mass Balance; MS: Mass Spectroscopy; N: Nitrogen; NOR: Nitrogen Oxidation Reaction; OA: Oxalic Acid; PCET: Proton-Coupled Electron Transfer; RHE: Reversible Hydrogen Electrode; STP: Standard Temperature and Pressure, TCD: Thermal Conductivity Detector; UEO: Urea Electro-Oxidation.

SYMBOLS

A_i : peak area obtained by GC analysis ($\mu\text{V}\cdot\text{min}$)

i : current density ($\text{A}\cdot\text{m}^{-2}$)

i^0 : initial current density ($\text{A}\cdot\text{m}^{-2}$)

I : intensity (A)

E_{consumed} : energy of the EC-cell (Wh)

\mathcal{F} : Faraday constant (96,500 C.mol⁻¹)

FE_i : Faraday efficiency of the compound i (%)

n_e : number of electrons (dimensionless)

n_i : amount of the compound i during electrolysis (mol)

$n_{i,\text{eq C}}$: carbon equivalent amount of the compound i during electrolysis (mol_C)

$n_{\text{eq C}}^{\circ}$: initial carbon equivalent amount of identified species (mol_C)

$n_{i,\text{eq N}}$: nitrogenous equivalent amount of the compound i during electrolysis (mol_N)

$n_{\text{eq N}}^{\circ}$: initial nitrogenous equivalent amount of identified species (mol_N)

$E_{\text{eq. H}_2 \text{ produced}}$: energy contained in H₂ gas at 25 °C and Patm (kWh)

Q_{total} : experimental amount of charge (C)

TOC: Total Carbon Organic Total (g.L⁻¹)

TOC_i: organic carbonaceous equivalent concentration of the compound i (gC.L⁻¹)

V_i : injected gaseous volume of the compound i (μL)

X: urea conversion rate (%)

ΔE : differential between energies consumed and equivalent produced by H₂ (Wh)

ΔV : cell voltage (V)

$\sum_i n_i$: sum of the respective quantities of the various compounds *identified* in the urine (mol)

λ_{H_2} : mass energy density (kWh.kg_{H₂}⁻¹)

REFERENCES

1. S. J. Yao, S. K. Wolfson, B. K. Ahn, and C. C. Liu, *Nature*, **241**, 471–472 (1973).
2. B. K. Boggs, R. L. King, and G. G. Botte, *Chem. Commun.*, 4859 (2009).
3. J. Li, J. Zhang, and J.-H. Yang, *Int. J. Hydrog. Energy*, **47**, 7693–7712 (2022).
4. D. Wang and G. G. Botte, *ECS Electrochem. Lett.*, **3**, H29–H32 (2014).
5. W. Simka, J. Piotrowski, and G. Nawrat, *Electrochimica Acta*, **52**, 5696–5703 (2007).
6. A. Abutaleb, *Catalysts*, **9**, 397 (2019).
7. H. Liu et al., *Nanoscale*, **13**, 1759–1769 (2021).
8. B. Zhu, Z. Liang, and R. Zou, *Small*, **16**, 1906133 (2020).
9. D. Zhu et al., *J. Mater. Chem. A*, **10**, 3296–3313 (2022).
10. X. Wang et al., *ChemCatChem*, **14**, e202101906 (2022).
11. G. Hopsort et al., *Electrochimica Acta*, **442**, 141898 (2023).
12. J. Li et al., *Angew. Chem. Int. Ed.*, **60**, 26656–26662 (2021).
13. S. W. Tatarchuk, J. J. Medvedev, F. Li, Y. Tobolovskaya, and A. Klinkova, *Angew. Chem.*, **134**, e202209839 (2022).
14. P. Wang et al., *Adv. Funct. Mater.*, 2300687 (2023).
15. W. Chen et al., *Angew. Chem. Int. Ed.*, **60**, 7297–7307 (2021).
16. G. Hopsort, L. Latapie, K. Groenen Serrano, K. Loubière, and T. Tzedakis, *AIChE J.*, e18113 (2023).
17. J. Kim, W. J. K. Choi, J. Choi, M. R. Hoffmann, and H. Park, *Catal. Today*, **199**, 2–7 (2013).
18. V. Amstutz, A. Katsaounis, A. Kapalka, C. Comninellis, and K. M. Udert, *J. Appl. Electrochem.*, **42**, 787–795 (2012).
19. G. Hopsort, L. Latapie, K. Groenen Serrano, K. Loubière, and T. Tzedakis, *Anal. Bioanal. Chem.* (2023).
20. K. T. Møller, T. R. Jensen, E. Akiba, and H. Li, *Prog. Nat. Sci. Mater. Int.*, **27**, 34–40 (2017).
21. E. Tzimas, C. Filiou, S. D. Peteves, and J.-B. Veyret, *Hydrogen Storage: State-of-the-Art and Future Perspective.*, JRC26493, (2003)
<https://publications.jrc.ec.europa.eu/repository/handle/JRC26493>.
22. Z. Shen, Y. Qi, W. Ge, H. Jiang, and C. Li, *Ind. Eng. Chem. Res.*, **0**, null.
23. N. Karki and S. W. Leslie, in *StatPearls.*, StatPearls Publishing, Treasure Island (FL) (2023)

<http://www.ncbi.nlm.nih.gov/books/NBK568783/>.

24. T. Brinkmann, G. Abbt-Braun, and F. H. Frimmel, *Acta Hydrochim. Hydrobiol.*, **31**, 213–224 (2003).
25. K. Carpenter and E. M. Stuve, *J. Appl. Electrochem.*, **51**, 945–957 (2021).
26. K. M. Hassan and M. Abdel Azzem, *J. Appl. Electrochem.*, **45**, 567–575 (2015).
27. S. Dbira, N. Bensalah, M. I. Ahmad, and A. Bedoui, *Materials*, **12**, 1254 (2019).
28. L.-C. Chen, T. Uchida, H.-C. Chang, and M. Osawa, *Electrochem. Commun.*, **34**, 56–59 (2013).
29. A. Schranck, R. Marks, E. Yates, and K. Doudrick, *Environ. Sci. Technol.*, **52**, 8638–8648 (2018).
30. T. Brinkmann, P. Hörsch, D. Sartorius, and F. H. Frimmel, *Environ. Sci. Technol.*, **37**, 4190–4198 (2003).
31. H. W. Schiwarra, H. Siegel, and A. Goebel, *Eur. J. Clin. Chem. Clin. Biochem. J. Forum Eur. Clin. Chem. Soc.*, **30**, 75–79 (1992).
32. A. Modvig and A. Riisager, *Catal. Sci. Technol.*, **9**, 4384–4392 (2019).
33. S. Bouatra et al., P. Dzeja, Editor. *PLoS ONE*, **8**, e73076 (2013).
34. G. H. El-Nowihy and M. S. El-Deab, *Renew. Energy*, **167**, 830–840 (2021).
35. D.-M. Zhou, H.-X. Ju, and H.-Y. Chen, *J. Electroanal. Chem.*, **408**, 219–223 (1996).
36. F. Franceschini and I. Taurino, *Phys. Med.*, **14**, 100054 (2022).
37. B. C. Tashie-Lewis and S. G. Nnabuiife, *Chem. Eng. J. Adv.*, **8**, 100172 (2021).